Journal of Business, Social and Technology
Volume 7, Issue 1, 110-119
e_ISSN: 2807-6362
https://bustechno.polteksci.ac.id/index.php/jbt/index
DOI: doi.org/10.59261/jbt.v7i1.592

Evaluation of the Effectiveness of CO_2 Nanobubbles as an Enhanced Oil Recovery Method on Low Permeability Artificial Core

***Softy Putri Adsura[1]**
Universitas Padjadjaran, Indonesia

Edy Sunardi[2]
Universitas Padjadjaran, Indonesia

***Corresponding author:**
Softy Putri Adsura, Universitas Padjadjaran, Indonesia. ✉softyadsura@gmail.com

Article Info:

Article history:
Received: December 01, 2025
Revised: January 03, 2026
Accepted: February 06, 2026

Keywords:
core flooding; enhanced oil recovery; low permeability; nanobubble CO_2; recovery factor; tight reservoir

Abstract

Background: Low-permeability reservoirs, characterized by limited pore connectivity and dominance of capillary forces, present significant challenges to conventional Enhanced Oil Recovery (EOR) methods. Water flooding often fails to mobilize residual oil in such reservoirs, which typically results in low recovery factors.
Objective: This study aims to evaluate the effectiveness of the Enhanced Oil Recovery (EOR) method based on CO_2 nanobubbles in low-permeability artificial cores with matrix-supported characteristics.
Methods: Experimental analysis was conducted on artificial cores fabricated from 80% quartz sand and 20% Portland cement. The study involved petrophysical characterization, oil saturation, and core flooding experiments using both water flooding and CO_2 nanobubble injection. Scanning Electron Microscopy (SEM) was used to observe microstructural changes and fluid redistribution.
Results: The initial characterization of the artificial core showed a porosity of ±31% and permeability of approximately 5 mD. Water flooding did not increase the recovery factor (RF = 0%), while CO_2 nanobubble injection achieved a recovery factor increase of ±3.76%. SEM observations revealed more uniform fluid redistribution and reduced residual oil after nanobubble flooding, confirming the effectiveness of CO_2 nanobubbles in mobilizing oil from tight pore systems.
Conclusion: The study concludes that CO_2 nanobubble-based EOR is effective in low-permeability reservoirs, with scale compatibility between nanobubble size and pore throat geometry playing a crucial role in enhancing recovery. This approach offers a promising direction for optimizing EOR in tight reservoirs.

To cite this article: Softy Putri Adsura, & Sunardi, E. (2026). Evaluation of the effectiveness of CO_2 nanobubbles as an enhanced oil recovery method on low permeability artificial core. *Journal of Business, Social and Technology*, 7(1), 110–119. https://doi.org/10.59261/jbt.v7i1.592

INTRODUCTION

Low permeability reservoirs (tight reservoirs) are one of the main challenges in oil and gas field development due to limited pore connectivity and the dominance of capillary forces in micro-to nano-sized pore systems (Ansyori, 2018; Gao et al., 2022; Nelson, 2009). Although some reservoirs have relatively good porosity, the small pore throat size causes limited fluid mobility, making the oil displacement process ineffective (Ahmed, 2018; Wang et al., 2024). As a result, conventional secondary recovery methods, such as waterflooding, often yield low sweep efficiency and leave significant amounts of residual oil (Chandra & Rachmat, 2018; Kristanto et al., 2018).

As an alternative, gas-based Enhanced Oil Recovery (EOR) methods, particularly CO_2 injection, have been widely developed due to their ability to reduce oil viscosity, increase fluid mobility, and improve oil displacement efficiency through oil swelling and miscibility mechanisms (Abdurrahman et al., 2016; Alvarado & Manrique, 2010; Burrows et al., 2020). However, in

reservoirs dominated by micropores and limited connectivity, conventional gas distribution tends to be uneven due to differences in capillary pressure and heterogeneity of flow paths, thus making the injection process suboptimal.

The limitations of conventional EOR in micropore systems are well-documented: conventional gas injection suffers from early breakthrough through high-permeability pathways, while waterflooding cannot overcome the capillary entry pressure required to displace oil from submicron pore throats (Abdurrahman et al., 2016). Recovery factors in tight reservoirs globally are estimated at 5–15%, compared to 35–45% in conventional reservoirs, highlighting the scale of the challenge (Seidy-Esfahlan et al., 2024). Despite extensive research on CO_2 EOR and nanoparticle-assisted EOR, a critical research gap remains: no study has systematically demonstrated geometric scale compatibility between injected bubble size and rock micropore throat dimensions as the primary determinant of EOR effectiveness in matrix-supported tight core systems (Abdurrahman et al., 2017). Recent micro-to nanoscale pore flow studies confirm that pore throat size distribution controls fluid mobilization more than porosity alone, yet this principle has not been experimentally validated using CO_2 nanobubbles.

The development of nanobubble technology offers a new approach in gas-based EOR applications. CO_2 nanobubbles have diameters on the nanometer scale, high stability in fluids, and a large specific surface area, thus potentially enhancing the interaction among the injected fluid, oil, and rock surface (Agarwal et al., 2011). The much smaller size of nanobubbles compared to conventional bubbles allows penetration into micropore systems and narrow pore throats, which generally dominate matrix-supported rocks (Lasek et al., 2023).

It is important to note that while CO_2 nanobubble technology has shown promising results at the laboratory scale, its direct application in real reservoir conditions remains at an early research stage, with field-scale validation yet to be established (Zheng et al., 2025). The novelty of the present approach lies in explicitly quantifying the geometric scale compatibility between nanobubble size and pore throat dimensions as the controlling EOR mechanism, distinguishing this study from prior works focused on chemical interaction effects such as wettability alteration and interfacial tension reduction.

Several previous studies have reported that CO_2 nanobubbles can affect fluid–rock interfacial properties, including wettability alteration, reduction of interfacial tension, and increased mobility of trapped fluids in fine-grained porous media (Bai et al., 2023; Yan et al., 2025). However, studies specifically linking nanobubble size with rock microstructure characteristics and their implications for enhancing the recovery factor are still limited, particularly in artificial core systems representing low permeability reservoirs.

Against this background, this study aims to experimentally evaluate the effectiveness of CO_2 nanobubble injection as an EOR method in low-permeability artificial cores, with a specific focus on elucidating the role of geometric scale compatibility between nanobubble size (507.3 nm) and micropore throat dimensions as the primary mechanism governing recovery improvement. The scientific novelty of this work lies in providing systematic experimental evidence that scale compatibility rather than chemical interaction alone is the dominant determinant of EOR effectiveness in matrix-supported tight reservoir analogs. This establishes a new conceptual framework for EOR injection strategy design in low-permeability formations, while acknowledging that the present study is a laboratory proof-of-concept requiring future field-scale validation.

METHOD

The research was conducted experimentally in the laboratory, comprising stages of artificial core fabrication, initial characterization, oil saturation process, core flooding experiments, and microstructural analysis using SEM.

Artificial Core Fabrication

The artificial core was made from a mixture of quartz sand (80%) and Portland cement (20%) with a grain size of 80 mesh. The mixture was homogenized, molded into a cylindrical shape, and dried until reaching a stable condition. The core dimensions were measured to determine the rock bulk volume.

The artificial core dimensions were: diameter 3.81 cm (1.5 inches) and length 7.62 cm (3 inches), bulk volume approximately 86.7 cm^3. After molding, cores were cured at 25°C for 28 days to achieve stable mechanical strength. Grain size uniformity was verified by sieve analysis prior to mixing to ensure reproducibility. The 80%/20% quartz sand–Portland cement composition replicates the matrix-supported texture of tight sandstone reservoirs with permeabilities in the 1–10 mD range.

Core Flooding Apparatus

The core flooding experiment was conducted using a fluid injection system consisting of an injection pump, core holder, pressure gauge, accumulator, and production separator. The apparatus used in this study is shown in Figure 1.

Core flooding parameters: injection rate 0.5 cc/min (ISCO 500D syringe pump), confining pressure 500 psi, back pressure 200 psi, temperature 30°C (±0.5°C, heating jacket). Flooding continued until a minimum of 5 pore volumes were injected (PVI) or cessation of oil production. Injection sequence: (1) brine saturation, (2) crude oil flooding for initial oil saturation (Soi), (3) water flooding at connate water saturation, (4) CO_2 nanobubble flooding post-water flooding. Differential pressure was monitored throughout all stages using a differential pressure transducer.

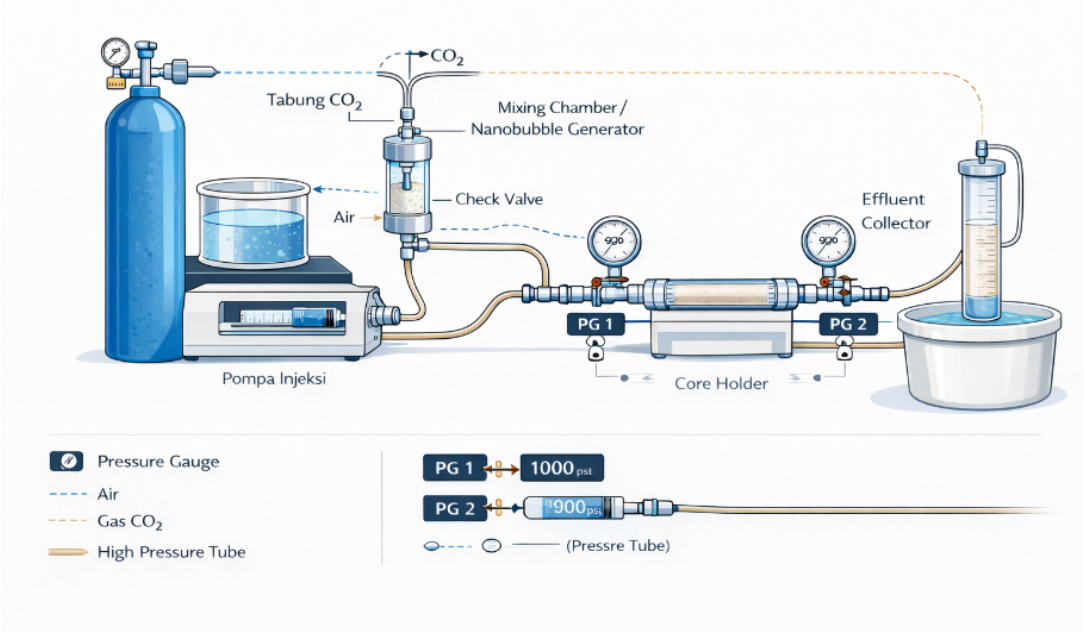

Figure 1. Core flooding apparatus used in the research.

CO_2 Nanobubble Preparation and Characterization: CO_2 nanobubbles were generated by pressurizing CO_2 gas into deionized water through a microporous membrane diffuser at 300 psi. Average hydrodynamic diameter: 507.3 nm (DLS, Malvern Zetasizer Nano ZS, 25°C), PDI = 0.23. Zeta potential: −23.4 mV. Concentration: ~1.2×10^8 bubbles/mL. Stability: >80% of initial concentration retained after 6 hours. All injections were performed within 2 hours of nanobubble preparation.

Initial Characterization

Petrographic analysis was conducted to identify the texture and rock type. The results showed that the sample is classified as Lithic Wacke with a matrix-supported texture, characterized by matrix dominance and limited pore connectivity.

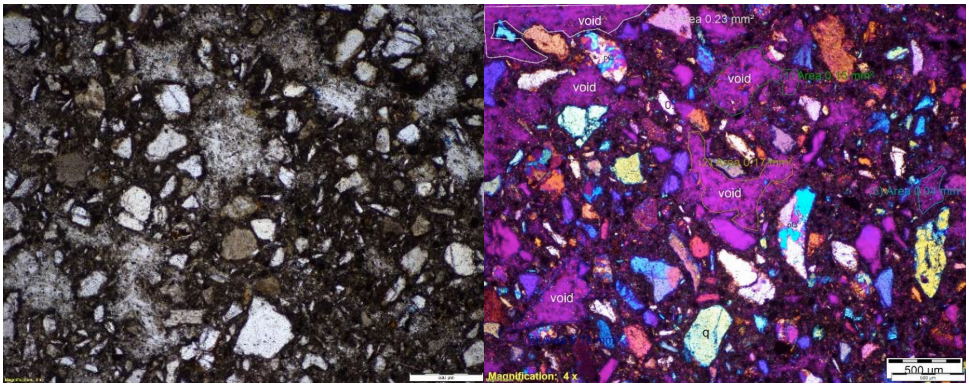

Figure 2. Petrographic analysis results for sample 9B2.1 after water flooding; Parallel Nicols (left), and Crossed Nicols (right).

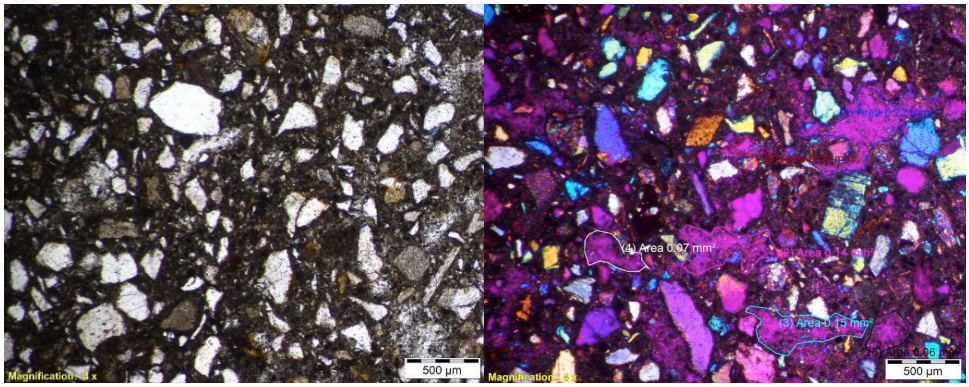

Figure 3. Petrographic analysis results for sample 9B3 after water flooding; Parallel Nicols (left), and Crossed Nicols (right).

Porosity measurement was carried out using the gravimetric method, while absolute permeability was measured based on Darcy's Law. The results showed an average porosity of ±31% and permeability of around 5 mD.

Saturation Process

The sample was evacuated to remove air from the pores, then saturated with synthetic oil until reaching initial oil saturation (Soi).

Figure 4. Oil Imbibition Process Using the Vacuum Method

Core Flooding

The experiment was conducted in two stages: 1) Water Flooding (Baseline): Water injection was carried out at a constant rate until no additional oil was produced. The Recovery

Factor was calculated as the ratio of the volume of oil produced to the initial oil volume. 2) CO_2 Nanobubble Flooding: CO_2 nanobubbles with an average size of 507.3 nm were injected under controlled operational parameters. The volume of additional oil produced was recorded to calculate the increase in RF.

SEM Analysis

Microstructural observations were conducted before and after flooding to evaluate changes in fluid distribution and pore space characteristics.

RESULT AND DISCUSSION

Result

This section presents experimental results from coreflooding experiments on low-permeability artificial cores, organized into: (1) petrophysical characterization, (2) waterflooding baseline, and (3) CO_2 nanobubble flooding results with SEM analysis. Recovery factor data for each phase are correlated with SEM observations to establish the mechanistic relationship between nanobubble size compatibility and pore-throat geometry. Mechanistic interpretation and scientific implications are presented in the Discussion subsection.

Petrophysical Characterization of Artificial Core

Tabel 1. Petrophysical Properties of Artificial Core.

Property	Value	Note
Porosity (phi)	31.2 ± 2.1 %	Values = averages of 3 replicate cores.
Permeability (k)	5.1 ± 0.8 mD	Permeability measured by N2 gas permeametry.
Bulk Volume	86.7 cm^3	
Pore Volume	27.1 cm^3	
Initial Oil Saturation (Soi)	67.3 %	
Connate Water Saturation (Swc)	32.7 %	
Grain Density	2.65 g/cm^3	
Core Diameter	3.81 cm	
Core Length	7.62 cm	

Initial measurement results showed that the artificial core made from a mixture of 80% quartz sand and 20% cement had an average porosity of ±31% and an absolute permeability of around 5 mD. This porosity value is considered moderate, but the low permeability indicates a pore system with limited connectivity. The matrix-supported texture (Figures 2 and 3) demonstrates the dominance of the matrix in controlling pore throat size.

This characteristic confirms that although the porosity is relatively high, the fluid transmission capacity remains limited by the geometry and distribution of pore throats. The waterflooding results showed no increase in recovery factor (RF). This indicates the dominance of capillary forces retaining residual oil in the micropore system. To evaluate microstructural changes due to the flooding process, analysis was conducted using a Scanning Electron Microscope (SEM).

Petrographic analysis showed that the sample is classified as a lithic wacke with a matrix-supported texture. The dominance of matrix in the intergranular space causes a reduction in pore throat size and contributes to the low fluid flow capacity. Narrow and unevenly distributed pore throats are the main characteristics of the low-permeability system in this sample.

Waterflooding Results (Baseline)

The waterflooding experiment was conducted at a constant injection rate until no additional oil production occurred. The calculation results showed no increase in the recovery factor (RF = 0%). The absence of additional oil production indicates that the injected water could not overcome the dominance of capillary forces in the micropore system. Residual oil remained

trapped within the narrow pore throats and intermatrix pores.

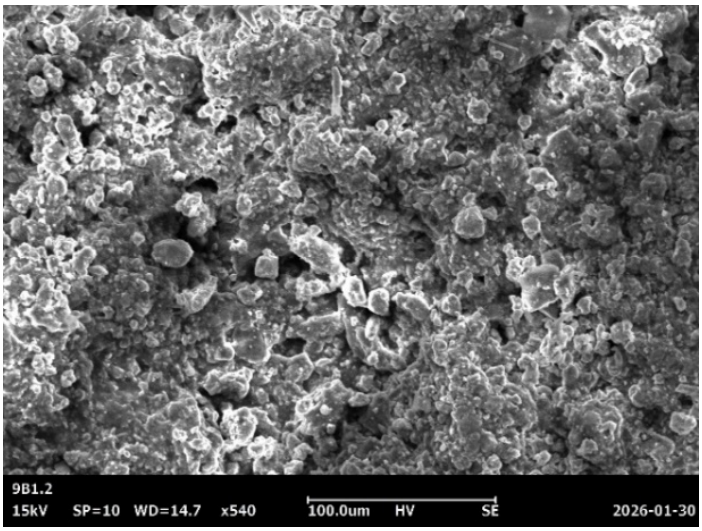

Figure 4. SEM image after water flooding shows the dominance of residual oil in the intergranular space

Observation results showed that the rock structure was still dominated by granular texture, with matrix filling the intergranular pore spaces. Pore throats appeared narrow with limited connectivity. No significant changes were observed in surface morphology or the opening of new flow paths after the water flooding process. Some intergranular spaces still appeared filled with material suspected to be residual oil or fine matrix.

This condition indicates that capillary forces still dominated the micropore system, so the injected water could not effectively mobilize residual oil. This finding is consistent with the recovery factor calculation results, showing an RF value of 0%. This finding confirms that the water displacement mechanism is ineffective in low-permeability systems with matrix-supported texture.

CO_2 Nanobubble Flooding Results

After water flooding, CO_2 nanobubble injection with an average size of 507.3 nm was carried out. The experimental results showed an increase in the recovery factor of ± 3.76%. The additional oil production obtained indicates that CO_2 nanobubbles were able to mobilize some of the previously trapped residual oil. After CO_2 nanobubble flooding, a more uniform fluid redistribution was observed in the intergranular pore spaces (Figure 5).

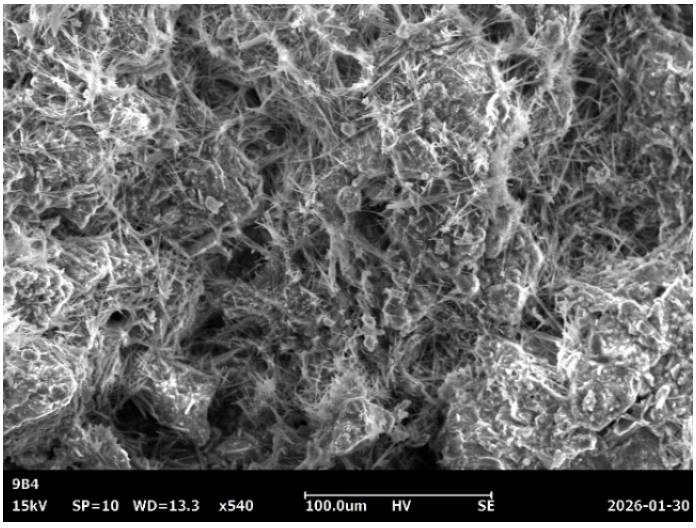

Figure 5. SEM image after CO_2 nanobubble flooding shows increased fluid distribution and indications of residual oil mobilization.

SEM observations after CO_2 nanobubble flooding showed a more uniform fluid distribution in the intergranular space compared to the post-water flooding condition. Indications of reduced residual oil accumulation were seen from the reduction in areas covered by discontinuous fluid material in the micropore system. Although no changes in grain morphology or formation of new flow paths were observed, a clear redistribution of fluid within the narrow pore-throat network was evident. This change indicates that the nanobubble size (507.3 nm) is compatible with the micropore-throat geometry, thereby enhancing penetration and sweep efficiency in the low-connectivity pore system. This finding suggests that CO_2 nanobubbles have a better capacity to mobilize residual oil compared to injected water in low-permeability artificial cores.

Research Novelty

The novelty of this research lies in three interconnected contributions. First, it provides systematic experimental evidence that geometric scale compatibility between CO_2 nanobubble size (507.3 nm) and micropore-throat geometry is the primary determinant of EOR effectiveness in matrix-supported tight reservoir analogs—a relationship theoretically proposed but not previously validated through controlled core flooding. Second, it quantitatively demonstrates that RF improvement of ±3.76% is achievable through size-compatible nanobubble injection where water flooding yields zero recovery, establishing a benchmark for future nanobubble EOR studies in tight formations. Third, the integration of DLS characterization, core flooding, and SEM within a single framework provides a replicable methodology for evaluating fluid-pore compatibility as an EOR design criterion.

Discussion

The characteristics of the artificial core used in this study show a combination of relatively high porosity (±31%) and low permeability (5 mD), reflecting a micropore system with limited connectivity. This condition is commonly encountered in low-permeability reservoirs, where the distribution and size of pore throats determine flow capacity more than the porosity value itself. The petrographic analysis results indicating a matrix-supported texture reinforce the interpretation that the matrix plays a dominant role in controlling fluid flow paths. The matrix filling the intergranular space causes throat narrowing and increases the dominance of capillary forces, so residual oil tends to be stably trapped within the pore system.

The absence of an increase in recovery factor during the water flooding stage (RF = 0%) indicates that the injection pressure and displacement mechanism by water were insufficient to overcome the capillary forces retaining residual oil. In low-permeability systems, injected water tends to flow through paths of least resistance without being able to effectively enter the micropore networ (Li et al., 2025). This leads to low sweep efficiency and the formation of bypassed oil zones. SEM observations after water flooding, which still showed the presence of residual oil in the intergranular space, further confirm that the conventional water flooding mechanism is inadequate for systems with narrow pore-throat geometry (Donaldson et al., 1985).

Conversely, the increase in recovery factor of ±3.76% after CO_2 nanobubble injection indicates an additional mechanism at play in mobilizing residual oil. The average nanobubble size of 507.3 nm falls within a range compatible with the scale of micropore throats in the artificial core, thus enabling penetration into pore spaces previously inaccessible to water. This scale compatibility is a crucial factor, because in tight reservoirs, fluid distribution is strongly influenced by the geometric relationship between the size of particles or bubbles and the throat size (Dake, 1983).

Besides the size compatibility factor, the presence of CO_2 also contributes to changes in fluid properties. CO_2 dissolved in oil has the potential to reduce viscosity and interfacial tension, thereby increasing the mobility of residual oil and the capillary number (Laini et al., 2014). An increased capillary number allows some of the previously capillary-trapped oil to be more easily mobilized. SEM observations after nanobubble flooding, which showed more uniform fluid redistribution in the intergranular space, support the interpretation that an increase in sweep efficiency occurred at the microscale.

Although the observed increase in recovery factor is still relatively moderate, this result has important implications for the development of EOR methods in low-permeability reservoirs.

This study confirms that the effectiveness of an EOR method is determined not only by the type of injected fluid but also by the compatibility between the physical characteristics of the fluid and the geometry of the rock pore system. A scale compatibility-based approach can serve as a conceptual foundation for designing more effective injection strategies for tight reservoirs, particularly in systems dominated by matrix-supported texture and complex micropore throats.

Scientific Contribution: The findings advance understanding of EOR mechanisms in tight systems by demonstrating that fluid-pore geometric compatibility is a prerequisite for effective oil mobilization, independent of chemical interaction effects alone. This positions pore-scale size matching as an equally critical design parameter alongside viscosity reduction and IFT alteration (Deng et al., 2023).

Practically, bubble size distribution relative to pore-throat size distribution should be incorporated as a standard step in EOR design for tight formations. Study Limitations: The use of artificial cores limits direct transferability to heterogeneous natural reservoir rock. Near-ambient conditions (30°C, 500 psi) do not replicate deep reservoir conditions where CO_2 is supercritical. The RF improvement of ±3.76% is a laboratory proof-of-concept, not a field-scale projection. Future research: (1) varying nanobubble sizes across different pore-throat distributions; (2) testing under supercritical CO_2 conditions; (3) nanobubble stability over extended PVI in porous media; (4) techno-economic feasibility of field-scale nanobubble generation.

CONCLUSION

This study provides experimental confirmation that CO_2 nanobubble-based EOR achieves measurable oil recovery improvement in low-permeability artificial cores where conventional water flooding is entirely ineffective. The artificial core system (porosity ~31%, permeability ~5 mD, matrix-supported texture) successfully replicated tight reservoir pore architecture, providing a controlled platform for mechanistic EOR investigation.

The central finding is that geometric scale compatibility between CO_2 nanobubble size (507.3 nm) and micropore throat geometry is the primary mechanism enabling oil mobilization in micropore-dominated systems. This advances EOR understanding in tight formations by identifying size-matching as a key design criterion. The RF improvement of ~3.76% through nanobubble injection versus 0% for water flooding demonstrates the fundamental advantage of scale-compatible EOR agents in overcoming capillary barriers in tight pore networks.

This work establishes the scale compatibility framework as a quantifiable approach for EOR agent selection in low-permeability reservoirs, supported by an integrated DLS–core flooding–SEM methodology. Future research should extend this to natural tight sandstone cores under reservoir pressure-temperature conditions, investigate varying nanobubble sizes against different pore throat distributions, and evaluate field-scale economic viability. The present results are confined to laboratory and artificial core systems; field-scale validation remains a critical next step.

ACKNOWLEDGEMENT

The authors would like to express their sincere gratitude to the Department of Petroleum Engineering, Universitas Padjadjaran, for providing laboratory facilities and technical support during the experimental stages of this research. The authors also appreciate the assistance of laboratory staff who contributed to the preparation of artificial core samples, core flooding experiments, and SEM analysis. Their support and cooperation greatly facilitated the successful completion of this study.

AUTHOR CONTRIBUTION STATEMENT

Softy Putri Adsura contributed to the conceptualization of the research, experimental design, data collection, laboratory experimentation, data analysis, and manuscript preparation. Edy Sunardi supervised the research process, provided methodological guidance, contributed to data interpretation, and reviewed and improved the manuscript critically. Both authors read and approved the final version of the manuscript.

REFERENCES

Abdurrahman, M., Bae, W., Novriansyah, A., & Khalid, I. (2016). Enhanced oil recovery (EOR) challenges and its future in Indonesia. *Proceeding of the IRES 28th International Conference*, *6*, 7–12.

Abdurrahman, M., Permadi, A. K., Bae, W. S., & Masduki, A. (2017). EOR in Indonesia: past, present, and future. *International Journal of Oil, Gas and Coal Technology*, *16*(3), 250–270.

Agarwal, A., Ng, W. J., & Liu, Y. (2011). Principle and applications of microbubble and nanobubble technology for water treatment. *Chemosphere*, *84*(9), 1175–1180. https://doi.org/10.1016/j.chemosphere.2011.05.054

Ahmed, T. (2018). *Reservoir engineering handbook*. Gulf professional publishing.

Alvarado, V., & Manrique, E. (2010). Enhanced oil recovery: an update review. *Energies*, *3*(9), 1529–1575. https://doi.org/10.3390/en3091529

Ansyori, M. R. (2018). Mengenal enhanced oil recovery (EOR) sebagai solusi meningkatkan produksi minyak. *Swara Patra: Majalah Ilmiah PPSDM Migas*, *8*(2), 16–22.

Bai, M., Liu, Z., Zhan, L., Yuan, M., & Yu, H. (2023). Effect of pore size distribution and colloidal fines of porous media on the transport behavior of micro-nano-bubbles. *Colloids and Surfaces A: Physicochemical and Engineering Aspects*, *660*, 130851. https://doi.org/10.1016/j.colsurfa.2022.130851

Burrows, L. C., Haeri, F., Cvetic, P., Sanguinito, S., Shi, F., Tapriyal, D., Goodman, A., & Enick, R. M. (2020). A literature review of CO2, natural gas, and water-based fluids for enhanced oil recovery in unconventional reservoirs. *Energy & Fuels*, *34*(5), 5331–5380.

Chandra, S., & Rachmat, S. (2018). Redefining EOR In Indonesia's Oil & Gas Industry: A Novel Solution to Overcome Lengthy Lag Time from EOR Implementation In Indonesia Post Gross Split Fiscal System. *Indonesian Journal of Energy*, *1*(2), 61–67.

Dake, L. P. (1983). *Fundamentals of reservoir engineering* (Vol. 8). Elsevier.

Deng, X., Kamal, M. S., Patil, S., Hussain, S. M. S., Mahmoud, M., Al-Shehri, D., & Al-Shalabi, E. W. (2023). Investigation of the coupled effect of IFT reduction and wettability alteration for oil recovery: New insights. *ACS Omega*, *8*(13), 12069–12078.

Donaldson, E. C., Chilingarian, G. V, & Yen, T. F. (1985). *Enhanced oil recovery, I: fundamentals and analyses*. Elsevier.

Gao, P., Feng, Q., Chen, X., Li, S., Sun, Y., Li, J., Zhou, J., & Qian, F. (2022). Numerical simulation and field application of biological nano-technology in the low-and medium-permeability reservoirs of an offshore oilfield. *Journal of Petroleum Exploration and Production Technology*, *12*(12), 3275–3288.

Kristanto, D., Harriyadi, H., Hermawan, Y. D., & Yusuf, Y. (2018). Studi Terintegrasi Kelayakan Proses Injeksi Gas CO2 untuk Enhanced Oil Recovery (EOR) di Lapangan Minyak. *Seminar Nasional Teknik Kimia" Kejuangan"*, 4.

Laini, R. E., Napoleon, A. N. A., & Munawar, M. (2014). Isolasi Bakteri Termofilik Penghasil Biosurfaktan yang Ber-potensi sebagai Agen MEOR (Microbial Enhanched Oil Re-covery) dari Sumur Minyak di Sungai Angit. *Jurnal Penelitian Sains*, *17*(1).

Lasek, L., Krzywanski, J., Skrobek, D., Zylka, A., & Nowak, W. (2023). Review of micro-and nanobubble technologies: advancements in theory and applications and perspectives on adsorption cooling and desalination systems. *Energies*, *16*(24), 8078.

Li, Y., Xu, H., Fu, S., Zhao, H., Chen, Z., Bai, X., Li, J., Xiu, C., Zhang, L., & Wang, J. (2025). Analysis of the effectiveness mechanism and research on key influencing factors of high-pressure water injection in low-permeability reservoirs. *Processes*, *13*(8), 2664.

Nelson, P. H. (2009). Pore-throat sizes in sandstones, tight sandstones, and shales. *AAPG Bulletin*, *93*(3), 329–340. https://doi.org/10.1306/10240808059

Seidy -Esfahlan, M., Tabatabaei-Nezhad, S. A., & Khodapanah, E. (2024). Comprehensive review of enhanced oil recovery strategies for heavy oil and bitumen reservoirs in various countries: Global perspectives, challenges, and solutions. *Heliyon*, *10*(18).

Wang, M.-J., Opoku, E. K., & Tham, A. (2024). Exploring Gen-Z consumers' preference for specialty coffee in the socio-cultural context of Taiwan. *Young Consumers*, *25*(3), 368–382.

Yan, W., Zhang, B., Yang, Y., Deng, J., & Li, W. (2025). The cavitation characteristics of micro–nanobubbles and their effects on the flotation recovery of fine-grained ilmenite. *Minerals*, *15*(6), 628.

Zheng, Z., Wang, X., Tang, T., Hu, J., Zhou, X., & Zhang, L. (2025). Properties of CO2 Micro-Nanobubbles and Their Significant Applications in Sustainable Development. *Nanomaterials*, *15*(16), 1270.